length of the interlamellar traverses the fraction of these traverses (F_t) must be known. This latter fraction can be obtained by a statistical "gambler's ruin" calculation.[21] Carrying out this calculation using input parameters for the sample prepared from material with $M_v = 5.9 \times 10^5$ by cooling to 0 °C and annealing at 30 °C gives 0.07. From the equation

$$\langle B \rangle = F_t \langle B \rangle_t + (1 - F_t)\langle B \rangle_0 \quad (7)$$

the average length of an interlamellar traverse, $\langle B \rangle_t$, for this sample is estimated as 30. However, this method predicts that F_t decreases with an increase in the noncrystalline content. This is unlikely since the noncrystalline content increases with molecular weight and therefore F_t increases with increasing noncrystalline content in this work.

Conclusions

The results of this study lead to the following conclusions:

1. The extent of reaction for TPI lamellas is dependent on the liquid medium used due to the possibility of crystal penetration from the lateral surfaces. Segmented block copolymers containing unreacted TPI sections and epoxidized TPI sections can be prepared by using 1-butanol as the reaction medium.

2. Tie molecules are detected in multilamellar TPI structures. The amount of these interlamellar linkages increases with increasing molecular weight.

3. The fraction of reacted double bonds determined by carbon-13 NMR is in good agreement with the fraction of the noncrystalline component from FTIR measurements and from density.

4. The average number of monomer unit per fold for the lamellas grown in this study is 9. The epoxidation results favor nearby reentry chain folding.

Acknowledgment is made to the donors of the Petroleum Research Fund, administered by the American Chemical Society, for support of this research. Support was also received from the PSC/CUNY Faculty Research Program and from the MBRS/NIH Program (Grant RN 08168).

Registry No. TPI, 9003-31-0.

References and Notes

(1) Schlesinger, W.; Leeper, H. M. *J. Polym. Sci.* **1953**, *11*, 203.
(2) Keller, A.; Martuscelli, E. *Makromol. Chem.* **1972**, *151*, 189.
(3) Anandakumaran, K.; Herman, W.; Woodward, A. E. *Macromolecules* **1983**, *16*, 563.
(4) Kuo, C.; Woodward, A. E. *Macromolecules* **1984**, *17*, 1034.
(5) Xu, J. R.; Woodward, A. E. *Macromolecules* **1986**, *19*, 1114.
(6) Communication with Dr. P. N. Chaturedi, whose paper will appear in *J. Mater. Sci., Lett. Ed.*
(7) Schilling, F. C.; Bovey, F. A.; Tonelli, A. E.; Xu, J. R.; Woodward, A. E., unpublished results.
(8) Schilling, F. C.; Bovey, F. A.; Anandakumaran, K.; Woodward, A. E. *Macromolecules* **1985**, *18*, 2688.
(9) Anandakumaran, K.; Kuo, C.; Mukherji, S.; Woodward, A. E. *J. Polym. Sci., Polym. Phys. Ed.* **1982**, *20*, 1669.
(10) Fisher, D. *Proc. Phys. Soc., London, Sect. B* **1953**, *66*, 7.
(11) Cooper, W.; Vaughan, G. *Polymer* **1963**, *4*, 329.
(12) Gavish, M.; Corrigan, J.; Woodward, A. E., submitted.
(13) Wunderlich, B. *Macromolecular Physics*; Academic: New York, 1973; Vol. 1.
(14) Tischler, F.; Woodward, A. E. *Macromolecules* **1986**, *19*, 1328.
(15) Chang, B. H.; Siegmann, A.; Hilter, A. *J. Polym. Sci., Polym. Phys. Ed.* **1984**, *22*, 255.
(16) Wang, P.; Woodward, A. E. *Macromolecules* **1987**, *20*, 1818.
(17) Wang, P.; Woodward, A. E. *Macromolecules* **1987**, *20*, 1823.
(18) Wagner, H.; Flory, P. J. *J. Am. Chem. Soc.* **1952**, *74*, 195.
(19) Mark, J. E. *J. Am. Chem. Soc.* **1967**, *89*, 6829.
(20) Mehta, A.; Wunderlich, B. *J. Makromol. Chem.* **1974**, *175*, 977.
(21) Gedde, U. W.; Jansson, J.-F. *Polymer* **1985**, *26*, 1469.

Electrochemical Doping Reactions of the Conducting Ladder Polymer Benzimidazobenzophenanthroline (BBL)

K. Wilbourn and Royce W. Murray*

Kenan Laboratories of Chemistry, University of North Carolina, Chapel Hill, North Carolina 27514. *Received May 17, 1987; Revised Manuscript Received July 16, 1987*

ABSTRACT: The electrochemical reactivity of films of the title polymer is examined by using cyclic voltammetry, coulometry, and spectroelectrochemistry. In contact with acidic aqueous $(Bu_4N)_2SO_4$ buffer, BBL voltammetry exhibits two redox steps corresponding to the sequential reduction of the unprotonated and the protonated forms of BBL connected by a $pK_a = 2.2$. The reductions consume overall one electron and one proton per BBL monomer site. The (more positive) reduction of unprotonated BBL is proposed to involve protonation at the carbonyl to yield a quinone/hydroquinone form; reduction of the protonated BBL is proposed to involve protonation of imine sites to yield a quinone/quinoimine form of the polymer. The quinone/quinoimine form is the more electrically conductive form of doped BBL.

The electrochemical reactivity of electrically conductive polymers[1] is an important aspect of their synthesis by electropolymerization, of their oxidation or reduction (i.e., doping) into a conducting state, of understanding their electronic structure, and of their application to energy storage or electrochromism.

This paper presents a study of the electrochemical reactivity of the polymer poly[(7-oxo-7*H*,12*H*-benz[*de*]-imidazo[4′,5′:5,6]benzimidazo[2,1-*a*]isoquinoline-3,4:11,12-tetrayl)-12-carbonyl], mercifully abbreviated BBL. This polymer is a member of the structurally diverse class of materials called ladder polymers, which are double-stranded, highly conjugated macromolecules. Ladder polymers have only recently experienced significant investigation;[2] there are now reports of significant electrical conductivities and other attractive properties such as liquid crystallinity and high thermal stability, to 500 °C in the case[3,4] of BBL.

0024-9297/88/2221-0089$01.50/0

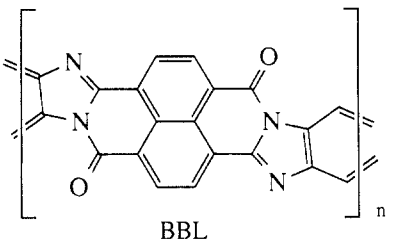

BBL

Data on BBL conductivity and electrochemical reactions have been previously reported by Kim[4] and Nowak et al.[5] Kim doped BBL chemically, with oxidants, reductants, and strong acids, and reports[4] σ_e electrical conductivities as high as 2 Ω^{-1} cm^{-1}. Nowak et al.[5] cast BBL films from methanesulfonic acid solutions and showed that BBL gives well-defined cyclic voltammetry and can be doped electrochemically. We undertook a further examination of BBL electrochemistry in the course of a study of the relationship of its conductivity to doping level and contacting solvent medium. We describe here coulometric, cyclic voltammetric, and spectroelectrochemical experiments relating to the central features of BBL electrochemical reduction reactions. Results dealing with BBL conductivity will be reported separately.[6]

Experimental Section

Chemicals. Acetonitrile (Burdick and Jackson spectral quality) was stored over molecular sieves; water was doubly distilled; supporting electrolytes were thrice recrystallized. Aqueous solutions of various pH were made by sequentially adding tetrabutylammonium hydroxide (40% aqueous, Aldrich) to sulfuric acid or vice versa. Sulfuric acid (MCB) and triethylamine (Aldrich) were used as received.

Preparation of Benzimidazobenzophenanthroline Ladder Polymer. Using a modified literature[7] preparation, 1,4,5,8-naphthalenetetracarboxylic acid (Aldrich) was reacted with 1,2,4,5-tetraaminobenzene tetrahydrochloride (Pfalz and Bauer) in Ar-degassed polyphosphoric acid for 24 h at 180 °C. The condensation polymer was precipitated from the reaction medium by pouring it into neutral water in a stirring blender. After filtration, the polymer was redissolved in methanesulfonic acid (Aldrich), reprecipitated in a stirring blender, refiltered, washed in a Soxhlet extractor with water until the washings were neutral, and dried in vacuo for 48 h at 120 °C. Elemental analysis suggested the presence of one residual water molecule: Anal. Calcd for $C_{20}H_6O_2N_4 \cdot H_2O$: C, 68.2; H, 2.27; N, 15.9; O, 13.6. Found: C, 68.2; H, 2.27; N, 15.3; O, 14.2.

Preparation of BBL Films on Electrodes. Films were prepared by spreading droplets of 2–4% w/w BBL solutions in methanesulfonic acid onto electrode surfaces followed by pumping off the solvent at 75 °C in vacuo. The films were neutralized by washing with a 10% triethylamine/ethanol solution and were redried in vacuo. These films, which were not yet doped and which exhibit low electrical conductivity (ca. 10^{-12} S/cm), have a deep purple color with a metallic sheen. Surface profilometry (Tencor Alpha-Step Model 100) on films analogously spread on flat glass was used to establish dry and wet film thicknesses, which were mostly in the range 1–10 μ with 4 μm being typical. Deposited film masses where needed were obtained by using a Cahn 29 electronic microbalance.

Electrochemistry. Cyclic voltammetry was performed in conventional three-electrode cells with NaCl-saturated calomel reference electrodes (SSCE) and Pt wire auxiliary electrodes. The working electrodes were either polished Pt disks (0.105 cm^2), polished glassy carbon disks (Tokai, 0.06 cm^2), or (for spectroelectrochemistry) highly doped SnO_2 films on glass plates. Spectroelectrochemistry was done with a Tracor Northern Model 1710 diode array spectrometer.

Results and Discussion

Cyclic Voltammetry of BBL in Aqueous Buffers. As reported by Nowak et al.,[5] the cyclic voltammetry of BBL films on (carbon or Pt) electrodes depends strongly on the solution pH. It also depends on the particular electrolyte ions present in the contacting solution. To examine the effect of pH independently of the effect of electrolyte composition, we varied the solution pH by mixing different combinations of aqueous $(Bu_4N)_2SO_4$, H_2SO_4, and Bu_4NOH solutions so that the final solution always contained at least 0.1 M $(Bu_4N)_2SO_4$. In observing the behavior of a given BBL film specimen over a series of pH values, the voltammetry was found to be the same whether the solution pH values were varied from high to low or vice versa. Results are shown in the series of steady-state voltammograms in Figure 1. Only reduction processes were observed starting from the synthetically prepared and cast films; no oxidations were seen out to solvent limits.

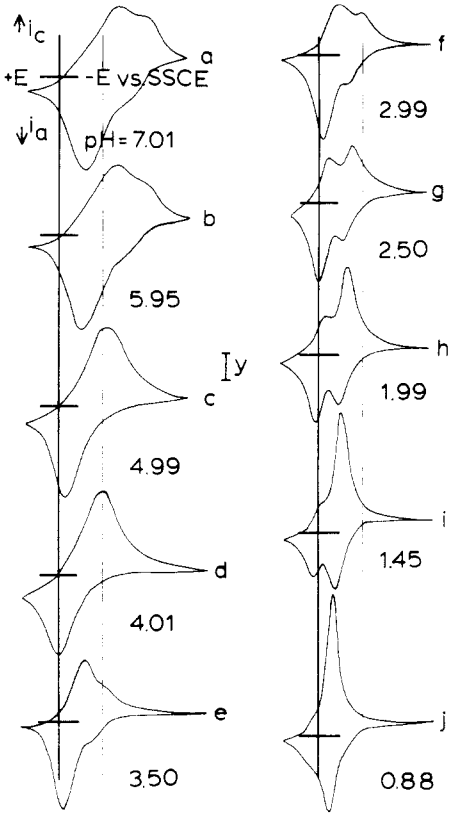

Figure 1. Cyclic voltammetry of BBL films on glassy carbon electrodes in aqueous media with 0.1 M $(Bu_4N)_2SO_4$ buffer. The dashed line is at −0.50 V vs. SSCE. Curves a–d were taken at 100 mV/s and y = 15 μA. Curves e–j were taken at 10 mV/s and y = 32 μA. Cathodic current is up and negative potentials are to the right.

The BBL voltammetric behavior divides into three regions of pH:

Region 1. Above pH 7 (up to 12), the voltammetric pattern changes very little with pH. The representative voltammogram in Figure 1a shows two waves: a main feature with formal potential (average of reduction and oxidation peak potentials) at −0.39 V versus SSCE and a poorly resolved smaller wave at ca. −0.84 V.

Region 2. Between pH 7 and 4, Figure 1b–d shows that the poorly resolved more negative wave disappears and the main wave shifts toward more positive potentials.

Region 3. At pH 4, only a single wave is evident, but with a substantial peak splitting (ΔE_p = 200 mV at 10 mV/s). At lower pH, the peak splitting diminishes and the wave shifts positively and divides into two waves, the more positive of which is largest at higher pH, the more negative wave being largest at lower pH. At pH ≤1, where the more negative wave is dominant, the current peaks in

Table I
BBL Coulometry

electrode	dry thickness (calcd), μm	coverage, mol/cm²	coulometry × 10⁻³, C	e⁻/mon. unit
Pt[a]	6.5	7.8 × 10⁻⁷	8.70	1.11
			7.58	0.96
Pt[a]	2.6	3.12 × 10⁻⁷	2.70	0.85
			2.95	0.93
			2.58	0.82
Pt[a]	4.0	4.69 × 10⁻⁷	4.92	1.04
			4.18	0.88
			4.83	1.02
			4.30	0.91
GC[b]	16.9	1.99 × 10⁻⁶	14.77	1.28
GC[b]	16.9	1.99 × 10⁻⁶	14.04	1.22
Pt*[c]	80.9	9.52 × 10⁻⁶	13.7	0.14
Pt*[c]	80.9	9.52 × 10⁻⁶	15.3	0.16
Pt*[c]	48.3	5.71 × 10⁻⁶	10.5	0.18
Pt[d]	4.0	4.69 × 10⁻⁷	5.29	1.11
			3.78	0.80

[a] pH 0.45; stepped from +0.5 to −0.175 V vs SSCE. [b] pH 7.04; stepped from +0.5 to −1.2 V vs SSCE. [c] pH 0.48; stepped from +0.5 to −0.175 V vs SSCE; *thickness too great for accurate measurement of charge. [d] 0.1 M Bu_4NClO_4/CH_3CN; stepped from 0.0 to −1.4 V vs SSCE.

the voltammetry are quite sharp and peak splitting is small (ΔE_p = 30 mV and E_{fwhm} = 118 mV). The voltammetric currents in region 3 are more stable than in regions 1 or 2 and are exceptionally robust at the lowest pH values. For example, the potential applied to a film in a pH 0.45 solution was cyclically scanned 10000 times over a 78-h period with no detectable change in the current–potential pattern.

Integrating the area under the voltammetric peaks (at slow potential scan rate the area was independent of scan rate) showed that the two voltammetric peaks in the region 3 pH range comprise a constant overall electrical charge. At higher pH, entering region 2, the charge under the overall voltammogram increases, apparently because of the appearance of the more negative wave. At pH 7 (Figure 1a), the overall voltammetric charge is 1.37 times that at pH 4.

The number of electrons involved in the BBL voltammetric reactions was further investigated by coating known weights of BBL on Pt disk electrodes and measuring the total charge accepted by the films in either slow potential sweeps or steps encompassing the voltammetric features shown in Figure 1. The results in acid solution and with thin (3–7 μm) BBL films show (Table I) that n = 1 in region 3; i.e., the polymer accepts on the average *one electron per monomer site* (using 334 g/mol as the monomer molecular mass).

For the BBL film used in the Figure 1j voltammetry, the results of Table I mean that 8 × 10⁻⁷ mol/cm² of the BBL monomer structural units are on the average each reduced by one electron in the voltammetric wave. Given the BBL dry density determined below, this amounts to the equivalent of reducing approximately 14000 monomer monolayers during the voltammetric sweep. This is a large quantity for such a sharp polymer film surface wave and must mean that electron and ion transport are both facile in this material at low pH.

It was observed that thicker coatings of BBL on the electrode led to electron/monomer values much less than unity (Table I, * values). It is clear that thick films do not readily charge as completely as thin ones. Whether this effect is due to counterion or electron transport limitations, or to a thickness-related polymer film morphology that places some sites in poor electrical contact with the electrode, was not investigated. All subsequent electrochemical experiments were done with thin films to avoid the problem. We should also note that the pH 7 Figure 1a voltammetric charge (vide infra) means that even for thin films delivery of a second electron into the BBL film occurs only to the extent of about one-third an electron/site. The reasons for this effect are not known, and we focus only on the behavior in the region 3 pH range.

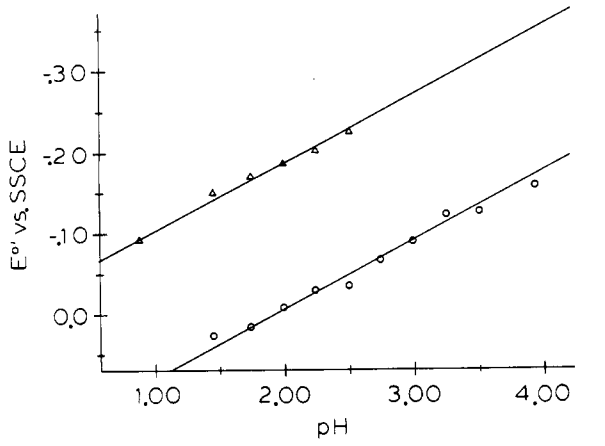

Figure 2. Pourbaix diagram of BBL reductions of protonated polymer (△) and unprotonated polymer (○) from pH 0.5–4.0 in 0.1 M $(Bu_4N)_2SO_4$ solution.

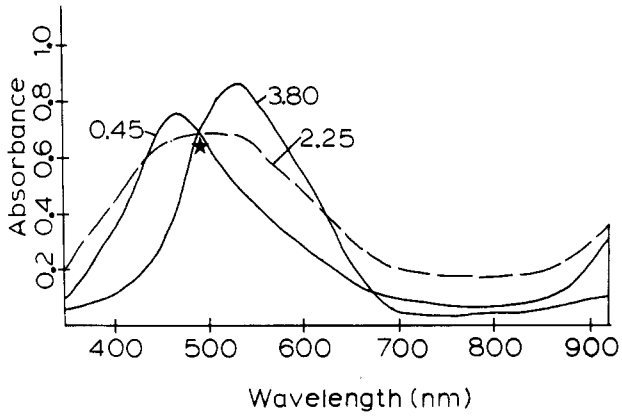

Figure 3. Spectra of BBL films on SnO_2/glass electrodes at indicated pH, with isosbestic point denoted.

Given that region 3 voltammograms exhibit a constant total charge (vide supra), the acid solution coulometry (Table I) shows that n = 1 throughout region 3. That is, the *two* voltammetric waves observed in region 3 (Figure 1e–j) comprise an *overall one-electron* process for the film. The pH effect implies then that an equilibrium exists between differently protonated structural units in the BBL film that have differing reduction potentials. As the pH changes, the relative portions of the differently protonated structural units change, and this is reflected in a change in the relative magnitudes of the two voltammetric peaks in region 3. What is unusual about this result is that the *protonated* structure has the more *negative* reduction potential. We will return to this point later.

The pH effect in region 3 can be further examined by plotting the formal potentials of the two voltammetric features (average of reduction and oxidation peak potentials) against pH (Figure 2). The lines shown both have slopes of 78 mV, which strictly speaking corresponds to reduction reactions that consume 1.3 protons per electron. Nowak et al.[5] cite 65 ± 7 mV for the more positive wave, which is closer to one proton/electron. To a first approximation we will take the two voltammetric BBL reduction reactions as being both one proton/electron steps.

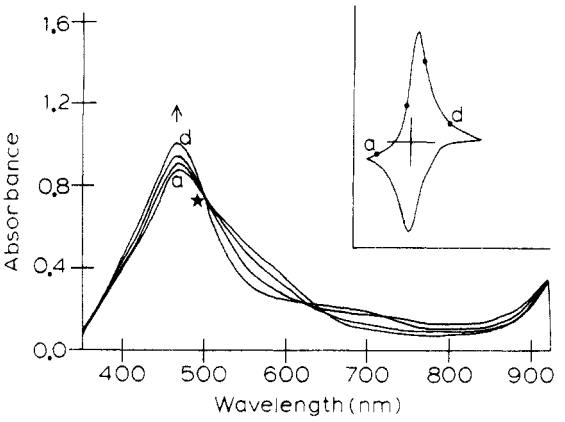

Figure 4. Spectroelectrochemistry of BBL film on conductive SnO_2 films on glass in pH 0.45 solution buffered by 0.1 M $(Bu_4N)_2SO_4/H_2SO_4$ with isosbestic denoted by ☆. Spectra a–d were taken at potentials as marked on cyclic voltammogram inset.

Spectroelectrochemistry of BBL Films in Aqueous Solution. Electronic absorption spectra (Figure 3) of BBL films not subjected to potential control confirm that BBL divides itself into differently protonated states over the region 3 pH interval. The basic, pH = 3.8 form exhibits a λ_{max} = 534 nm, the pH 0.45 protonated form absorbs at λ_{max} = 466 nm, and a definite isosbestic point occurs at 494 nm. The spectra are quite stable and the pH changes are quantitatively reversible. The midpoint of the spectral change lies at about pH 2.2, which agrees quite well with the Figure 1 voltammetry where the two voltammetric peaks are of approximately equal size at this pH (interpolate between parts g and h of Figure 1).

These results show that BBL undergoes protonation in aqueous $(Bu_4N)_2SO_4$ solutions with an *average* pK_a of about 2.2. We note on the other hand that both the Figure 1 voltammetric and Figure 3 spectral changes are perceptible over a wider (ca. 3 pH units) pH span than might be expected for a single simple pK_a value. This problem may also contribute to the deviation of the proton/electron slope in Figure 2 from the ideal 60-mV value. We speculate that the wide pH span may reflect the known[8] tendency of polyelectrolyte acid and bases to exhibit site–site interactions that cause a gradual shift in effective pK_a as the molecule becomes more highly charged. That is, it is plausible that the individual base sites in BBL gradually become slightly less strongly basic at lowered pH as more and more of their neighbors become protonated and highly polycationic. Other possible factors could be isomeric diversity (vide infra), chain end groups, and/or uncyclized (defect) units.

Transmission spectra of BBL films on optically transparent SnO_2 electrodes equilibrated at various potentials (i.e., doped to different levels) are shown in Figures 4–6 for solutions of pH 0.5, 2.25, and 7.01, respectively. The points on the voltammogram inserts in the figures indicate the potentials at which the films were equilibrated before collecting the spectra, in each case proceeding from positive to negative potentials. In general, the BBL spectra show intense absorption ($\epsilon > 25\,000$) between 400 and 550 nm with weaker absorption in the region 600–800 nm. Another strong absorption is seen in the near-IR (not shown). The strong peaks are presumably strongly allowed transitions shifted to low energies by the extended, conjugated BBL structure.

Figure 4 corresponds to reduction of the more or less completely protonated state BBL film. The initial spectrum is the same as in Figure 3, with λ_{max} = 466 nm. The fully reduced state shows an increase in intensity but no shift in λ_{max} and a broad absorption near 690 nm. A clean isosbestic point at 497 nm and a less well defined one near 630 nm are consistent with predominance of a single overall electrochemical reaction, proceeding from a protonated, oxidized BBL state to a single reduced product with an additional one electron and one proton.

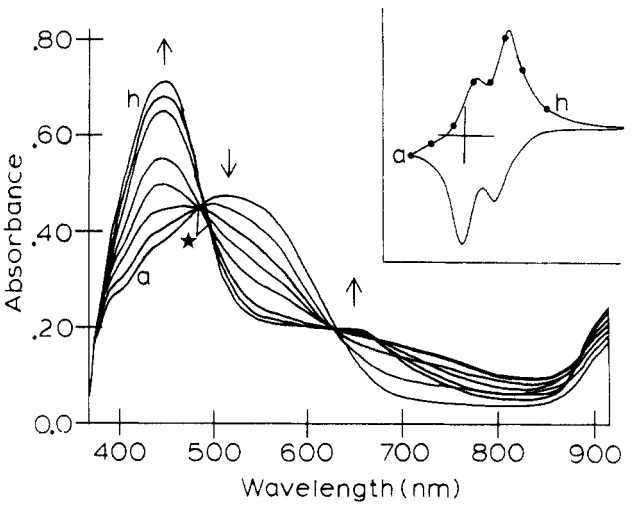

Figure 5. Spectroelectrochemistry of BBL film on conductive SnO_2 films on glass in pH 1.99 solution buffered by 0.1 M $(Bu_4N)_2SO_4/H_2SO_4$ with isosbestics denoted by ☆. Spectra a–h were taken at potentials as marked on the cyclic voltammogram inset.

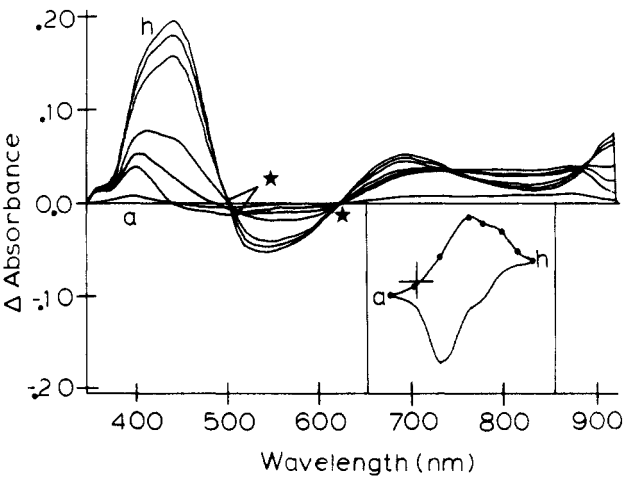

Figure 6. Difference spectroelectrochemistry of BBL film on conductive SnO_2 films on glass in pH 7.01 solution buffered with 0.1 M $(Bu_4N)_2SO_4$. Spectra a–h were taken at potentials as marked on the cyclic voltammogram insets with isosbestics denoted by ☆.

Spectroelectrochemistry (Figure 5) for reduction of a film at pH 2.25, where approximately half of the BBL sites are protonated, is more complex, but it is possible to pick out two distinct changes associated with the two voltammetric waves. The first four spectral traces (starting at curve a) are taken at potentials which span the first voltammetric wave (reduction of the unprotonated species). These spectra show increase and decrease in absorbances at 446 and 514 nm, respectively, and an isosbestic point at 484 nm. In the last four spectra (ending at h), which cross the second voltammetric feature (reduction of the protonated state), the 446-nm peak continues to grow, but the isosbestic point shifts to 497 nm which is the same as that observed for the protonated species in Figure 4. There is again a broad absorption at 660 nm.

Comparison of Figures 4 and 5 shows that while reduction of protonated BBL produces little change in the

Chart I

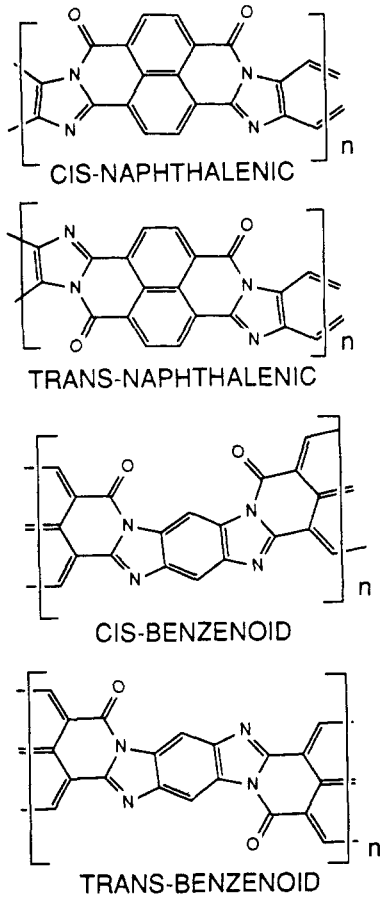

spectrum around 466 nm (Figure 4), reduction of unprotonated BBL produces a much more pronounced, blue shift in λ_{max}. That is, the absorbance growing at 446 nm in Figure 4 must present an unresolved overlap of the absorbances of the reduced forms of protonated (absorbs at 466 nm) and unprotonated (must absorb at 446 nm or lower) BBL. Reduction of initially unprotonated BBL is accompanied by protonation, and so in this sense by reference to Figure 3 a blue shift is expected.

Spectroelectrochemistry at higher pH (regions 1 and 2) shows little change with pH; Figure 6 shows spectra at pH 7.01 as difference spectra relative to the unreduced film. There is an increase in absorbance first at 404 nm and then at 444 nm, accompanied by isosbestic points at 513 and 501 nm, respectively. A weaker broad absorbance grows at 685 nm and becomes well defined as the second voltammetric peak is crossed.

A Proposed Scheme for BBL Electrochemical Reactions. We present next a proposal for the molecular features of the protonation and electrochemical reactions of BBL. It is apparent that the molecular problem is a somewhat complex one. We regard the proposed scheme as a reasonable accommodation of the experimental facts, but clearly more structurally sensitive spectroscopic experiments are needed to make it firm.

Consider first some important steric aspects of synthetic assembly of the BBL chain structure, shown in Chart I. Two different cis–trans stereochemistries might result during the condensation reaction; both the naphthalenic and the benzenoid units can condense with the amide carbonyls being either cis or trans with respect to one another. The possible existence of isomers from the condensation complicates interpretation, but further consideration of the structures shows three of them are equivalent in terms of the stabilizing resonance structures which

Chart II

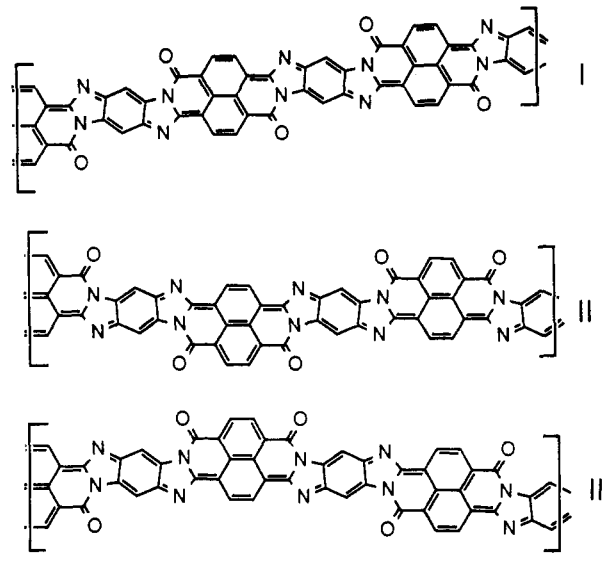

can be drawn, with the cis-benzenoic isomer being different. Condensation to produce the trans-benzenoic, trans-naphthalenic, and cis-naphthalenic structures allows for each a resonance structure including a quinone–imine resonance form and a quinodimethane resonance form in the naphthalenic unit. Neither of these resonance structures is possible in the cis-benzenoic isomer. Thus if the condensation is thermodynamically rather than kinetically controlled, the favored forms are trans-quinoid and possibly a mixture of cis- and trans-naphthalenic. That is, the BBL preparation should consist (Chart II) of [(trans)quinoid–(trans)naphth–(trans)quinoid–(trans)naphth], I, [(trans)quinoid–(cis)naphth–(trans)quinoid–(cis)naphth], II, or [(trans)quinoid–(cis)naphth–(trans)quinoid–(trans)naphth], III.

Consider next the BBL protonation chemistry in light of these structures. We concluded from Figure 3 that oxidized BBL exhibits an average pK_a of 2.2. Of the base sites available, the imine site is more plausibly associated with a pK_a of this magnitude than is the amide carbonyl. Imine protonation is proposed to effect the λ_{max} 534 to 466 nm blue shift seen in Figure 3. The broad pH range of the protonation process mentioned above might also be associated with slightly different pK_a's for isomers I, II, and III. With the isomer structure I as an example, Chart III shows an imine-protonated BBL structure, IV, in equilibrium with unprotonated I, adding one proton per monomer repeat unit.

Chart III also presents the proposed one electron/one proton electrochemical reduction of unprotonated BBL (couple I,V) and of protonated BBL (couple IV,VI) at low pH (region 3 in Figure 1). The principal variables in the scheme are the sites for protonation in V and VI. In that connection, we should recall the unusual feature of the voltammetry that in region 3 it appears that the protonated species IV has a more negative reduction potential than the unprotonated BBL. It is very common in organic electrochemistry that protonation results in states that are more readily (rather than less readily) reduced.[9]

To rationalize this departure from the usual pattern of organic reductions, we propose that the protonation occurs at *different sites* within the BBL structure in the one electron/one proton reduction of I → V versus the one electron/one proton reduction of IV → VI. Chart III depicts reduction and further protonation of protonated BBL (the IV,VI couple) to result in uniform protonation of the imine nitrogens and consequent quinoimine and quinone

Chart III

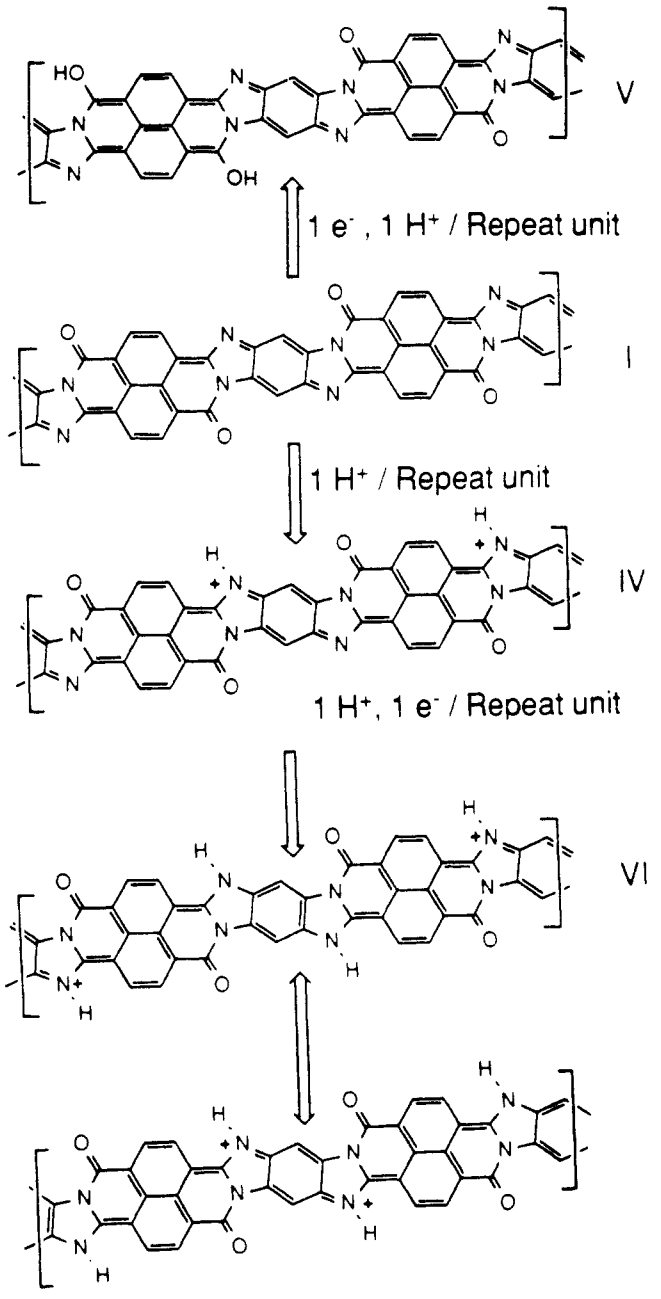

resonance forms. Reduction and consequent protonation of the initially unprotonated BBL (the I,V couple) is on the other hand depicted to result in protonation at the carbonyl oxygens with consequent alternating quinone and hydroquinone resonance forms. The higher energy transition (466 nm) is associated with both initially protonated BBL and with the reduction products of the more negative voltammetric wave, and the less protonated BBL is associated with the 534-nm transition and the more positive of the two waves.

The proposal in Chart III corresponds in the case of the reduced, protonated form of BBL (VI) to a structure that has a strong parallel to the highly conducting form of polyaniline proposed recently[10] by MacDiarmid in his "proton doping" studies. That is, for electrical conductivity along the BBL chain, a cationically charged imine site can be "moved" to a different imine nitrogen simply within the context of structurally equivalent resonance forms (see bottom of Chart III).

We predict then, in comparison with structure V, that structure VI should be the more highly (electrically) conducting one. This indeed is what we observe[6] in conductivity measurements (to be reported elsewhere). That is, in region 3 where two voltammetric features are visible, the increase in conductivity observed upon reduction of the film at the potential of the second wave (the IV → VI process) is greater than that observed for reduction at the potential of the first wave (the I → V process).

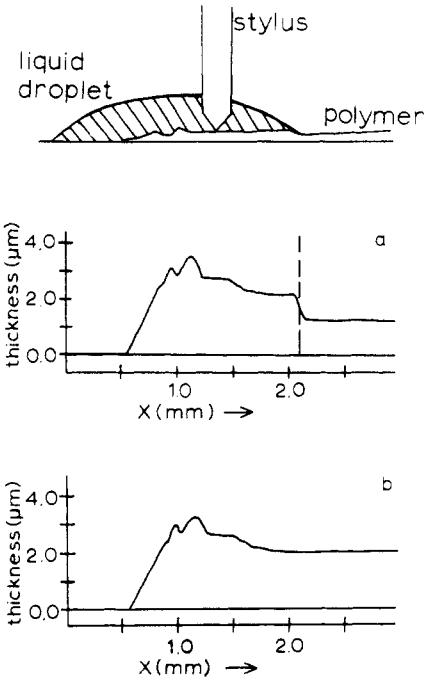

Figure 7. Surface profile of the edge of a "dry" BBL film on glass substrate (a) with a droplet of aqueous H_2SO_4 extending between $x = 0$ and dashed line; (b) same profile with the droplet covering the entire polymer film.

BBL Film Swelling. BBL film thicknesses were assessed by surface profilometry as shown in Figure 7. We established by subsequent microscopy that in the present experiments the force exerted by the profiler probe does not cause furrowing in the BBL film.

In the upper panel (Figure 7a), a droplet of aqueous H_2SO_4 (pH 0.5) was placed at the edge of the film so as to cover part of the smooth glass substrate, the rough edge of the film, and a portion of the more smooth interior of the film. The profilometer trace shows a rise from the smooth glass substrate surface over a "coastal range" that is typical of the outer edges of polymer films formed from relatively rapidly evaporated solution droplets. The surface profile shows a smooth polymer surface in the interior of the film, until the needle probe encounters the edge of the H_2SO_4 droplet, whereupon a decrease in the polymer film thickness is sensed followed again by a smooth, dry surface.

In Figure 7b, the H_2SO_4 droplet was spread over a larger portion of the film interior, so that the probe is run over only wetted film. The thickness change seen in Figure 7a is by this result definitely traced to the droplet's edge, since it disappears in the Figure 7b profile.

The surface profiles in Figure 7 allow determination of the densities of air-dry and pH 0.5 wetted BBL films. The air-dry BBL film has a density of 0.39 g/cm^3 which corresponds to a monomer site concentration of 1.2 M. The pH 0.5 wetted film has a density of 0.18 g/cm^3 which is a monomer site concentration of 0.54 M. These density and concentration determinations include any void spaces or surface texture too fine (<10 μm) to be interrogated by the profilometer tip, which has a 12.5-μm radius. The substantial swelling (218%) that BBL undergoes in contact

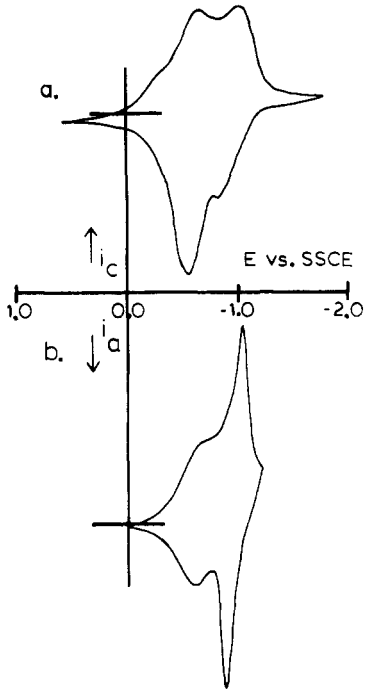

Figure 8. Cyclic voltammetry of BBL film on Pt disk electrodes (100 mV/s) in Ar-saturated (a) 0.1 M Bu_4NClO_4/CH_3CN and (b) 0.1 M Et_4NClO_4/CH_3CN.

with the acidic droplet is most likely associated with the increased ionic character given the polymer by the BBL protonation reaction discussed above. Among the possible reasons for the changes in voltammetric peak splitting and width seen in Figure 1 throughout region 3 are that the enhanced ionic conductivity leads to the decreased ΔE_p peak splitting and the diminished site–site interactions in the swollen film leads to the decreased peak width (E_{fwhm}).

Electrochemistry of BBL Films in Acetonitrile. Voltammetric studies in acetonitrile were of interest both because it allows quenching of protonic equilibria and because it revealed strong electrolyte charge interaction effects of potential importance to understanding BBL conductivity.[6] BBL films are reduced at more negative potentials in acetonitrile than in water, as expected since the aqueous reactions consume protons that are unavailable in the aprotic solvent. The films are less well swollen in acetonitrile and the voltammetry is highly variable depending on the electrolyte employed as illustrated in Figure 8. The result with Et_4NClO_4 agrees with that reported[5] by Nowak et al. In general two waves are observed although with some electrolytes ($LiClO_4$, for example) one or two additional indistinct shoulders also appear. It is expected that BBL reduction should be accompanied for reasons of electroneutrality by ingress of supporting electrolyte cations into the film, and it apparently matters a great deal whether the cation is Et_4N^+ or Bu_4N^+.

The results of coulometric reductions (Table I) of films in acetonitrile show that the sum of the charge under the voltammetric waves in Figure 8 again amounts to one electron per monomer site. This is analogous to the behavior in pH region 3 in aqueous electrolyte where two waves also appear, i.e., Figure 1, but of course protonic equilibria cannot cause the wave splitting in acetonitrile. It may be that both the wave splitting and its strong dependence on electrolyte cation reflect a strong charge localization on the BBL chain by the compensating cation (e.g., Et_4N^+ versus Bu_4N^+). A possible reduction process is shown in Chart IV, leading to quinodimethane-like states that are strongly resonance stabilized.

Chart IV

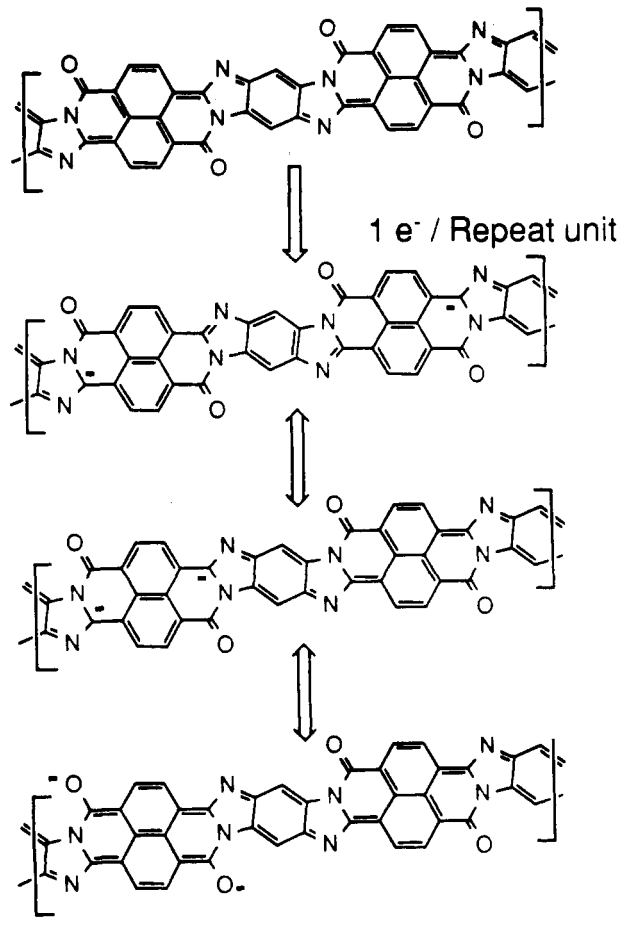

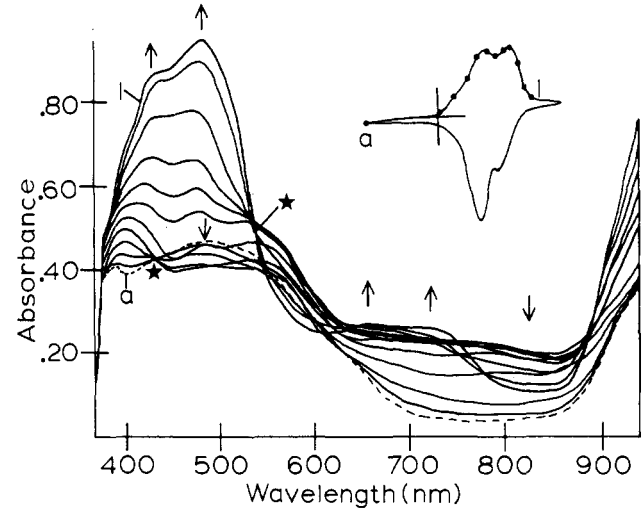

Figure 9. Spectroelectrochemistry of BBL film on conductive SnO_2 films on glass in 0.1 M Bu_4NClO_4/CH_3CN. Spectra a–i were taken at potentials as marked on the cyclic voltammogram inset with isosbestics denoted by ☆. The spectrum of unreduced BBL is shown as (---).

Spectroelectrochemistry in Acetonitrile. The potential dependence of the spectrum of a BBL film on a SnO_2 electrode is documented in Figure 9. The unreduced film (---) exhibits a peak at 485 nm which (see arrow) decreases as the applied potential passes over the first voltammetric feature; simultaneously an absorbance at 400 nm grows in, with an isosbestic point at 428 nm. As the potentials cross the second voltammetric feature, the optical density of the film increases greatly with peaks at 433 and 479 nm growing in, with a second isosbestic point at

538 nm. Broad absorbances also appear at longer wavelength in the 650–700-nm range and in the near-IR. The primary information from these spectra is that the two voltammetric reductions involve spectrally distinguishable species, and so the multiple voltammetric peaks are unlikely to simply arise from morphological swelling heterogeneity within the film.

Acknowledgment. This research was supported in part by grants from the National Science Foundation and the Office of Naval Research.

Registry No. I, 36900-46-6; C, 7440-44-0; Pt, 7440-06-4; $SnCl_2$, 18282-10-5; (1,4,5,8-naphthalenetetracarboxylic acid)(1,2,4,5-tetraaminobenzene) (copolymer), 110851-60-0; 1,4,5,8-naphthalenetetracarboxylic acid, 128-97-2; 1,2,4,5-tetraaminobenzene tetrahydrochloride, 4506-66-5.

References and Notes

(1) (a) *Handbook of Conducting Polymers*; Skotheim, T. A., Ed.; Marcel Dekker: New York, 1986; Vol. 1, 2. (b) Frommer, J. E.; Chance, R. R. *Encyclopedia of Polymer Science and Engineering*, 2nd ed.; Wiley: New York, 1986; Vol. 5, pp 462–507.
(2) (a) Ruan, J. Z.; Litt, M. H. *J. Polym. Sci., Polym. Chem. Ed.* **1987**, *25*, 285. (b) Ruan, J. Z.; Litt, M. H. *Synth. Met.* **1986**, *15*, 237. (c) Iqbal, Z.; Maleysson, C.; Baughman, R. H. *Synth. Met.* **1986**, *15*, 161. (d) Litt, M. H.; Ruan, J. Z. *Polym. Mater. Sci. Eng.* **1986**, *55*, 731. (e) Chien, J. C. W.; Carlini, C. *J. Polym. Sci., Polym. Chem. Ed.* **1985**, *23*, 1383. (f) Bizzarri, P. C.; Della Casa, C. *Mol. Cryst. Liq. Cryst.* **1985**, *118*, 245. (g) Young, C. L.; Whitney, D.; Vistnes, A. I.; Dalton, L. R. *Annu. Rev. Phys. Chem.* **1986**, *37*, 459. (h) Kim, O. K. *J. Polym. Sci., Polym. Lett. Ed.* **1985**, *23*, 137.
(3) (a) Berry, G. C. *J. Poly. Sci., Polym. Symp.* **1978**, *65*, 143. (b) Berry, G. C. *Discuss. Faraday Soc.* **1970**, *49*, 121.
(4) (a) Kim, O. K. *J. Polym. Sci., Polym. Lett. Ed.* **1982**, *20*, 663. (b) Kim, O. K. *Mol. Cryst. Liq. Cryst.* **1984**, *105*, 161.
(5) Polyak, L.; Rolison, D. R.; Kessler, R. J.; Nowak, R. J. 163rd Meeting of the Electrochemical Society; San Francisco, May 8–13, 1983; Extended Abstracts 547, 1983.
(6) Wilbourn, K. O.; Murray, R. W., submitted for publication.
(7) (a) Van Densen, R. L.; Gorns, A. K.; Surei, A. J. *J. Poly. Sci., Polym. Chem. Ed.* **1968**, *6*, 1777. (b) Arnold, F. E.; Van Densen, R. L., *Macromolecules* **1969**, *2*, 497.
(8) Perrin, D. D.; Dempsey, B.; Serjeant, E. P. *pK_a Predictions of Organic Acids and Bases*; Chapman and Hall: London, 1981.
(9) Baizer, M. M.; Lund, H., Eds. *Organic Electrochemistry*; Marcel Dekker: New York, 1983.
(10) (a) MacDiarmid, A. G.; Chaing, J.-C.; Halpern, M.; Huang, W.-S.; Mu, S.-L.; Somasiri, N. L. D.; Wu, W.; Yaniger, S. I. *Mol. Cryst. Liq. Cryst.* **1985**, *121*, 173. (b) MacDiarmid, A. G.; Chang, J. C.: Huang, W. S.; Humphrey, B. D.; Somasiri, N. L. D. *Mol. Cryst. Liq. Cryst.* **1985**, *125*, 309.

Single-Ion Conduction in Poly[(oligo(oxyethylene) methacrylate)-*co*-(alkali-metal methacrylates)]

Eishun Tsuchida,* Norihisa Kobayashi, and Hiroyuki Ohno

Department of Polymer Chemistry, Waseda University, Tokyo 160, Japan.
Received April 9, 1987; Revised Manuscript Received July 1, 1987

ABSTRACT: Thin films of poly[(oligo(oxyethylene) methacrylate)-*co*-(alkali-metal methacrylates)] were prepared from methanol solutions of oligo(oxyethylene) methacrylate and alkali-metal methacrylates by casting and polymerization on a Teflon plate under nitrogen. The ionic conductivity of the films depends on the electrolyte content, the dissociation energy of the alkali-metal methacrylate, and the degree of motion of polymer segments surrounding the ions in the polymer matrix. The ionic conductivity of the polymeric Li and K salts is 10^{-6} S/cm at 80 °C. The transient ionic current after reversing the dc bias polarity shows one sharp peak corresponding to cation migration, indicating that the polymer is a cationic single-ion conductor. The temperature dependence of conductivity was determined. The Williams–Landel–Ferry parameters, calculated from the temperature dependence of conductivity, agreed reasonably well with theoretical values, confirming the influence of polymer segmental motion on conductivity. Additional confirmation was obtained from a Vogel–Tammann–Fulcher plot.

Introduction

Polymeric solid electrolytes with high ionic conductivity are of interest in theoretical and basic research as well as for the development of novel devices. Matrix polymers for such electrolytes include an organic polar polymer/additive system,[1-3] polyether,[4-15] poly(ethylene succinate),[16,17] poly(ethyleneimine),[18] and poly(alkylene sulfide).[19] Combinations of these matrices with $LiClO_4$ show ionic conductivities of 10^{-6}–10^{-9} S/cm at 25 °C. Ionic conductivity as high as 10^{-5} S/cm in the system poly[oligo(oxyethylene) methacrylate]/LiX[13] is attributed to the flexible oligo(oxyethylene) segment, which has a lower glass transition temperature than crystalline poly(oxyethylene). Comblike polymers containing similar oligo(oxyethylene) chains have been used as matrix polymers.[20-23] Shriver et al. report that the hybrid system [polyphosphazene with an oligo(oxyethylene) side chain]/AgO_3SCF_3 has a conductivity of about 10^{-3} S/cm at 70 °C.[20]

However, since these matrices are bi-ion conductors, their ionic conductivities decrease with continued dc voltage even though alkali-metal nonblocking electrodes are used. This problem is attributed to the localization of counteranions near the anode, which inhibits the supply of alkali-metal cations from it. This decrease in dc conductivity prevents the use of such systems in devices driven under dc polarization. Accordingly, a single-ion conductive matrix is required for such uses as dry batteries, sensory systems, and capacitors. Polyelectrolytes should provide such single-ion conductive matrices because the opposite charges are fixed on the polymer chains. However, alkali-metal salts of such polyanions as poly(methacrylic acid) and poly(styrenesulfonic acid) are essentially insulators in the dry state, presumably because their T_g is too high for ionic conduction at ambient temperature and because they contain no segment that promotes salt dissociation. One approach to a single-ion conductor involves blending polyelectrolyte salts with soft segments such as poly(oxyethylene), which renders cations mobile. Selective ion conduction in such blends can be attributed to the relatively larger diffusion constants of small ions compared to those of giant polyions. Another approach involves introduction into a polymer matrix of structural units with

0024-9297/88/2221-0096$01.50/0